iJRASET
International Journal For Research in Applied Science and Engineering Technology

INTERNATIONAL JOURNAL FOR RESEARCH

IN APPLIED SCIENCE & ENGINEERING TECHNOLOGY

Volume: 8 **Issue:** IV **Month of publication:** April 2020

DOI: http://doi.org/10.22214/ijraset.2020.4080

www.ijraset.com

Call: 08813907089 | E-mail ID: ijraset@gmail.com

International Journal for Research in Applied Science & Engineering Technology (IJRASET)
ISSN: 2321-9653; IC Value: 45.98; SJ Impact Factor: 7.429
Volume 8 Issue IV Apr 2020- Available at www.ijraset.com

Unique Solution of Unpolarized Evolution Equations

Dr. Ranjt Baishya
J. N. College, Boko, Kamrup, Assam, Assam - 781123

Abstract: ***The singlet and non-singlet structure functions have been obtained by solving DGLAP evolution equations in leading order (LO) at the small-x limit. A Taylor series expansion has been used and then the method of characteristics to solve the evolution equations. Also calculated t and x evolutions of deuteron as well as non-singlet (combination of proton and neutron) structure functions and the results are compared with the New Muon Collaboration (NMC), E665, CLAS and NNPDF collaboration data.***

I. INTRODUCTION

The high-energy lepton-nucleon scattering has served as a sensitive probe for the substructure of the proton and neutron. Experiments with high energy electrons, muons and neutrinos have been used to characterize the parton substructure of the nucleon and to establish the current theory of the strong interaction □□□quantum chromodynamics. Observations of the experiments are scaling violation for the unpolarized nucleon structure functions, the measurement of the strong coupling constant $\alpha_S\left(Q^2\right)$, the confirmation of numerous QCD sum rules and the extraction of the parton distributions inside the nucleon. The parton distribution functions (PDFs) depend on two kinematical variables x and Q^2. Their Q^2 dependence is called scaling violation, which is calculated by the DGLAP evolution equations [1-4] in the perturbative QCD region. The Q^2 evolution equations are frequently used in describing high-energy hadron reactions. Because the PDFs vary significantly in the current accelerator-reaction range, Q^2=1 GeV^2 to 10^5 GeV^2, the Q^2 dependence should be calculated accurately.

It is well known that all information about the structure of hadrons participating in DIS comes from the hadronic structure functions. According to QCD, at small values of x and at large values of Q^2 hadrons consist predominately of gluons and sea quarks. In that region, the DGLAP evolution equations give t [= ln (Q^2/Λ^2), Λ is the QCD cut off parameter] and x evolutions of structure functions. Hence the solutions of DGLAP evolution equations give quark and gluon structure functions that produce ultimately proton, neutron and deuteron structure functions.

The solutions of the unpolarized DGLAP equation for the quantum chromodynamics evolution of parton distribution functions have been discussed considerably over the past years [5-13]. But exact analytical method with unique solution is not known. Here we will solve unpolarized DGLAP evolution equations analytically by using method of characteristics and get unique solutions. Our results are compared with various experimental data.

A. Theory

The DGLAP evolution equations [1-4] in matrix form

$$\frac{\partial}{\partial \ln Q^2}\begin{pmatrix} F_2^S \\ G \end{pmatrix} = \begin{pmatrix} P_{qq} & P_{qg,} \\ P_{gq} & P_{gg} \end{pmatrix} \otimes \begin{pmatrix} F_2^S \\ G \end{pmatrix}, \qquad (1)$$

where F_2^S and G are singlet and gluon structure functions respectively and $P_{qq}, P_{qg}, P_{gq}, P_{gg}$ are splitting functions. For evolution of singlet structure function, the quark-quark splitting function P_{qq} and gluon-quark splitting function P_{qg} have to be calculated and for non-singlet structure function, we have to calculate only quark-quark splitting function P_{qq}, which can be expressed as [13]

$$P_{qq}\left(x,Q^2\right) = \frac{\alpha_S\left(Q^2\right)}{2\pi} P_{qq}^{(0)}(x) + \left(\frac{\alpha_S\left(Q^2\right)}{2\pi}\right)^2 P_{qq}^{(1)}(x) + \left(\frac{\alpha_S\left(Q^2\right)}{2\pi}\right)^3 P_{qq}^{(2)}(x) + \cdots$$

where $P_{qq}^{(0)}(x)$, $P_{qq}^{1}(x)$ and $P_{qq}^{(2)}(x)$ are LO, NLO and NNLO splitting functions respectively. Again $\otimes$ represents the standard Mellin Convolution with the notation

$$a(x)\otimes b(x)\equiv\int_0^1\frac{dy}{y}a(y)b\left(\frac{x}{y}\right). \qquad (2)$$

Similarly, other splitting functions can be expressed.

The strong coupling constant, $\alpha_S(Q^2)$ is related with the β-function [13] as

$$\beta(\alpha_S)=\frac{\partial\alpha_S(Q^2)}{\partial\log Q^2}=-\frac{\beta_0}{4\pi}\alpha_s^2-\frac{\beta_1}{16\pi^2}\alpha_s^3-\frac{\beta_2}{64\pi^3}\alpha_S^4+\cdots,$$

with

$$\frac{\alpha(Q^2)}{2\pi}=\frac{2}{\beta_0 t}\left[1-\frac{\beta_1}{\beta_0^2}\frac{\log t}{t}+\frac{1}{\beta_0^3 t}\left\{\frac{\beta_1^2}{\beta_0}(\log^2 t-\log t-1)+\beta_2\right\}+O\left(\frac{1}{t^3}\right)\right],$$

$$\beta_0=\frac{11}{3}N_C-\frac{4}{3}T_f,$$

$$\beta_1=\frac{34}{3}N_C^2-\frac{10}{3}N_C N_f-2C_F N_f,$$

$$\beta_2=\frac{2857}{54}N_C^3+2C_F^2T_f-\frac{205}{9}C_F N_C T_f-\frac{1415}{27}N_C^2T_f+\frac{44}{9}C_F T_f^2+\frac{158}{27}N_C T_f^2,$$

where N_c is the number of colour, N_f is the number of active flavour and T_f, C_F are constants associated with the colour SU(3) group. We have set $N_C = 3$, $C_F=\frac{N_C^2-1}{2N_C}=\frac{4}{3}$ and $T_f=\frac{1}{2}N_f$. Here β_0,β_1 and β_2 are the one loop, two loop and three loop corrections to the QCD β - function. We can neglect β_1 and β_2 in LO. Considering splitting functions [14, 15, 16], the DGLAP evolution equations for singlet and non-singlet structure functions in LO in standard form are

$$\frac{\partial F_2^S}{\partial t}-\frac{\alpha_S(t)}{2\pi}\frac{2}{3}\left[\{3+4\ln(1-x)\}F_2^S(x,t)+I_1^S(x,t)+I_2^S(x,t)\right]=0, \qquad (3)$$

$$\frac{\partial F_2^{NS}}{\partial t}-\frac{\alpha_S(t)}{2\pi}\frac{2}{3}\left[\{3+4\ln(1-x)\}F_2^{NS}(x,t)+I_1^{NS}(x,t)\right]=0, \qquad (4)$$

Here $\frac{\alpha_S(t)}{2\pi}=\frac{3A_f}{2t}$ with $A_f=\frac{4}{33-2N_f}$ and functions I_1^S, I_2^S, I_1^{NS} are defined as

$$I_1^S(x,t)=2\int_x^1\frac{d\omega}{1-\omega}\left[(1+\omega^2)F_2^S\left(\frac{x}{\omega},t\right)-2F_2^S(x,t)\right]$$

$$I_2^S(x,t)=2N_f\int_x^1\{\omega^2+(1-\omega)^2\}G\left(\frac{x}{\omega},t\right)d\omega\quad I_1^{NS}(x,t)=2\int_x^1\frac{d\omega}{1-\omega}\left[(1+\omega^2)F_2^{NS}\left(\frac{x}{\omega},t\right)-2F_2^{NS}(x,t)\right]$$

Let us introduce the variable u = 1 − ω and note that

$$\frac{x}{\omega}=\frac{x}{1-u}=\left(x+\frac{xu}{1-u}\right) \qquad (5)$$

ISSN: 2321-9653; IC Value: 45.98; SJ Impact Factor: 7.429
Volume 8 Issue IV Apr 2020- Available at www.ijraset.com

Since $x<\omega<1$, so $0<u<1$ $\square\square$ x and hence the series (3.5) is convergent for $|u|<1$.

So, we can use Taylor's series expansion in $F_2^S\left(\frac{x}{\omega},t\right)$, $F_2^{NS}\left(\frac{x}{\omega},t\right)$ and $G\left(\frac{x}{\omega},t\right)$ as

$$F_2^S\left(\frac{x}{\omega},t\right)=F_2^S\left(x+\frac{xu}{1-u},t\right)$$

$$=F_2^S(x,t)+\frac{xu}{1-u}\frac{\partial F_2^S(x,t)}{\partial x}+\frac{1}{2}\left(\frac{xu}{1-u}\right)^2\frac{\partial^2 F_2^S(x,t)}{\partial^2 x}+\cdots\cdots,$$

$$G\left(\frac{x}{\omega},t\right)=G(x,t)+\frac{xu}{1-u}\frac{\partial G(x,t)}{\partial x}+\frac{1}{2}\left(\frac{xu}{1-u}\right)^2\frac{\partial^2 G(x,t)}{\partial^2 x}+\cdots\cdots,$$

$$F_2^{NS}\left(\frac{x}{\omega},t\right)=F_2^{NS}(x,t)+\frac{xu}{1-u}\frac{\partial F_2^{NS}(x,t)}{\partial x}+\frac{1}{2}\left(\frac{xu}{1-u}\right)^2\frac{\partial^2 F_2^{NS}(x,t)}{\partial^2 x}+\cdots\cdots.$$

Since x is small in our region of discussion, the terms containing x^2 and higher powers of x can be neglected and we can rewrite

$$F_2^S\left(\frac{x}{\omega},t\right)\approx F_2^S(x,t)+\frac{xu}{1-u}\frac{\partial F_2^S(x,t)}{\partial x}, \qquad (6a)$$

$$G\left(\frac{x}{\omega},t\right)\approx G(x,t)+\frac{xu}{1-u}\frac{\partial G(x,t)}{\partial x}, \qquad (6b)$$

$$F_2^{NS}\left(\frac{x}{\omega},t\right)\approx F_2^{NS}(x,t)+\frac{xu}{1-u}\frac{\partial F_2^{NS}(x,t)}{\partial x}. \qquad (6c)$$

Here if we introduce the higher order terms in Taylor's expansion, then also there is no modification of the solution. Because when we solve the second order partial differential equation by Monges Method [17], which will be produced by introducing the second order terms in Taylor expansion, then ultimately it becomes the first order as before due to the form of the DGLAP equation. Similarly by introducing more terms in Taylor expansion, we hope for these cases also the terms can be neglected due to still smaller values of x [18-21].

Using equations (6a) and (6b) and performing u-integrations we get

$$I_1^S(x,t)=\{-3+2x+x^2\}F_2^S(x,t)+\{x-x^3-2x\ln(x)\}\frac{\partial F_2^S(x,t)}{\partial x}, \qquad (7a)$$

$$I_2^S(x,t)=2N_f\left[\left(\frac{2}{3}-x+x^2-\frac{2}{3}x^3\right)G(x,t)+\left(-\frac{5}{2}x+3x^2-2x^3+\frac{2}{3}x^4-x\ln(x)\right)\frac{\partial G(x,t)}{\partial x}\right]. \qquad (7b)$$

Putting equations (7a) and (7b) in equation (3) we get

$$\frac{\partial F_2^S(x,t)}{\partial t}-\frac{\alpha_s}{2\pi}\left[A_1(x)F_2^S(x,t)+A_2(x)\frac{\partial F_2^S(x,t)}{\partial x}+A_3(x)G(x,t)+A_4(x)\frac{\partial G(x,t)}{\partial x}\right] \qquad (8)$$

where $A_1(x)=2x+x^2+4\ln(1-x)$, $A_2(x)=x-x^3-2x\ln(x)$,

$A_3(x)=2N_f\left(\frac{2}{3}-x+x^2-\frac{2}{3}x^3\right)$ and $A_4(x)=2N_f\left(-\frac{5}{3}x+3x^2-2x^3+\frac{2}{3}x^4-x\ln(x)\right)$.

In order to solve equation (8), we need to relate the singlet structure function $F_2^S(x,t)$ with the gluon structure function $G(x,t)$. For small-x and high-Q^2, the gluon is expected to be more dominant than the sea quark. But for lower-Q^2, there is no such clear cut distinction between the two [18, 22]. Hence for simplicity, let us assume

$$G(x,t) = k(x) F_2^S(x,t), \quad (9)$$

where k(x) is a suitable function of x or may be a constant. Here we may assume k(x) = k, ax^b, ce^{dx} where k, a, b, c and d are suitable parameters which can be determined by phenomenological analysis. But the possibility of the breakdown of relation also can not be ruled out [18, 21, 22]. Now equation (8) gives

$$-t\frac{\partial F_2^S(x,t)}{\partial t} + L_1(x)\frac{\partial F_2^S(x,t)}{\partial x} + M_1(x)F_2^S(x,t) = 0, \quad (10)$$

where

$$L_1(x) = A_f[(A_2 + kA_4)], \quad (11a)$$

$$M_1(x) = A_f\left[\left(A_1 + kA_3 + \frac{\partial k}{\partial x}A_4\right)\right]. \quad (11b)$$

To introduce Method of characteristics, let us consider two new variables S and τ instead of x and t, such that

$$\frac{dt}{dS} = -t, \quad (12a), \qquad \frac{dx}{dS} = L(x), \quad (12b)$$

which are known as characteristic equations [23]. Again according to the rule of PDE we have

$$\frac{dt}{dS}\frac{\partial F_2^S(x,t)}{\partial t} + \frac{dx}{dS}\frac{\partial F_2^S(x,t)}{\partial x} = \frac{dF_2^S(x,t)}{dS}.$$

Thus putting equations (12a) and (12b) in equation (10), we get

$$\frac{dF_2^S(S,\tau)}{dS} + M_1(S,\tau)F_2^S(S,\tau) = 0 \quad (13)$$

Then equation (13) gives $\frac{dF_2^S(S,\tau)}{F_2^S(S,\tau)} = -M_1(S,\tau)dS$, which can be solved as

$$F_2^S(S,\tau) = F_2^S(0,\tau)\exp\left[-\int_0^S M_1(S,\tau)dS\right]. \quad (14)$$

For t-evolution, structure function varies with t remaining x constant [22]. Thus the equation (14) becomes $F_2^S(S,\tau) = F_2^S(\tau)\left(\frac{t}{t_0}\right)^{M_1(S,\tau)}$ with the initial condition: when $S = 0$ then $t = t_0$ and $F_2^S(S,\tau) = F_2^S(0,\tau)$. Now we have to replace the co-ordinate system (S, τ) to (x, t) with the input function $F_2^S(0,\tau) = F_2^S(x,t_0)$ and will get the t-evolution of singlet structure function in LO as

$$F_2^S(x,t) = F_2^S(x,t_0)\left(\frac{t}{t_0}\right)^{M_1(x)}. \quad (15)$$

Similarly for x-evolution, structure function varies with x remaining t constant. Thus the equation (14) becomes $F_2^S(S,\tau) = F_2^S(S)\exp\int -\frac{M_1(S,\tau)}{L_1(S,\tau)}dx$ with the initial condition: when τ = 0 then $x = x_0$ and $F_2^S(S,\tau) = F_2^S(S,0)$. Now we have to replace the co-ordinate system (S, τ) to (x, t) with the input function $F_2^S(S,0) = F_2^S(x_0,t)$ and will get the x-evolution of singlet structure function in LO as

$$F_2^S(x,\ t) = F_2^S(x_0, t)\exp\int_{x_0}^{x} -\frac{M_1(x)}{L_1(x)}dx \ . \qquad (16)$$

Proceeding in the same way, we get t and x evolutions of non-singlet structure function from equation (3.4) as

$$F_2^{NS}(x,t) = F_2^{NS}(x,t_0)\left(\frac{t}{t_0}\right)^{A_f A_1(x)} \qquad (17a)$$

$$F_2^{NS}(x,\ t) = F_2^{NS}(x_0, t)\exp\int_{x_0}^{x} -\frac{A_1(x)}{A_2(x)}dx \ . \qquad (17b)$$

The deuteron, proton and neutron structure functions measured in DIS can be written in terms of singlet and non-singlet quark distribution functions [15] as

$$F_2^d(x,\ t) = \frac{5}{9}F_2^S(x,\ t), \qquad (18a)$$

$$F_2^p(x,t) = \frac{5}{18}F_2^S(x,t) + \frac{3}{18}F_2^{NS}(x,t), \qquad (18b)$$

$$F_2^n(x,t) = \frac{5}{18}F_2^S(x,t) - \frac{3}{18}F_2^{NS}(x,t). \qquad (18c)$$

Thus

$$F_2^{NS}(x,t) = 3\left[2F_2^p(x,t) - F_2^d(x,t)\right], \qquad (18d)$$

$$F_2^{NS}(x,t) = 3\left[F_2^p(x,t) - F_2^n(x,t)\right]. \qquad (18e)$$

The t and x-evolution of deuteron structure functions in LO can be obtained by putting equations (15) and (16) respectively in the equation (18a) as

$$F_2^d(x,\ t) = F_2^d(x,\ t_0)\left(\frac{t}{t_0}\right)^{M_1(x)}, \qquad (19a)$$

$$F_2^d(x,\ t) = F_2^d(x_0, t)\exp\int_{x_0}^{x} -\frac{M_1(x)}{L_1(x)}dx \ , \qquad (19b)$$

where

$$F_2^d(x,t_0) = \frac{5}{2}F_2^S(x,t_0), \qquad (20a)$$

$$F_2^d(x_0,t) = \frac{5}{2}F_2^S(x_0,t). \qquad (20b)$$

Equations (19a) and (19b) are used in our phenomenological work for deuteron structure function and equations (17a) and (17b) are used for non-singlet structure function which is the combination of proton and deuteron or neutron related by the relations (18d) or (18e).

ISSN: 2321-9653; IC Value: 45.98; SJ Impact Factor: 7.429
Volume 8 Issue IV Apr 2020- Available at www.ijraset.com

II. RESULTS AND DISCUSSIONS

Here we compare our results of t and x-evolution of deuteron structure function $F_2^d(x,t)$ as well as non-singlet structure function $F_2^{NS}(x,t)$ measured by the NMC in muon-deuteron DIS [24], Fermilab E665 data in muon-deuteron DIS [25], CLAS Collaboration from the CEBAF Large Acceptance Spectrometer (CLAS) at the Thomas Jefferson National Accelerator Facility [26, 27] as well as NNPDF Collaboration [28, 29 30] based on Artificial Neural Networks by considering their parameterization from NMC and BCDMS [31] data. We consider the QCD cut-off parameter $\Lambda_{\overline{MS}} = 0.323$ GeV for $\alpha_S(M_Z^2) = 0.119 \pm 0.002$ [32]. In all plots, solid curves are our best fit results. Experimental data and parameterization are given with vertical upper and lower error bars for total uncertainties of statistical and systematic errors. Structure functions at lowest-Q^2 for t-evolutions and at largest-x for x-evolutions are taken as input functions.

The NMC data consist of four data sets for the proton and the deuteron structure functions corresponding to beam energies of 90 GeV^2, 120 GeV^2, 200 GeV^2 and 280 GeV^2. They cover the kinematics range $0.002 \le x \le 0.60$ and $0.5\ GeV^2 \le Q^2 \le 75\ GeV^2$. Again E665 data were taken at Fermilab in inelastic muon scattering with average beam energy of 470 GeV^2. Similarly in CLAS Collaboration data, measurement of the deuteron structure function from the inclusive cross sections measured in interactions of electrons with a liquid deuterium target. The data cover Q^2 values from 0.4 to 6 GeV^2. The data are taken from the CLAS internal note from Osipenka et al. The authors combine these data with other world data to study the Q^2 evolution of its moments and higher twist effects [26]. On the other hand, the BCDMS data consist of four data sets for the proton structure function, corresponding to beam energies of 100 GeV^2, 120 GeV^2, 200 GeV^2 and 280 GeV^2 and three data sets for the deuteron structure function corresponding to beam energies of 120 GeV^2, 200 GeV^2 and 280 GeV^2. They cover the kinematic range of $0.06 \le x \le 0.80$ and $7\ GeV^2 \le Q^2 \le 280\ GeV^2$. For our phenomenological work, we consider the ranges as $0.0045 \le x \le 0.180$ and $0.75\ GeV^2 \le Q^2 \le 48.0\ GeV^2$ for NMC data, $0.01 \le x \le 0.069$ and $1.496\ GeV^2 \le Q^2 \le 13.391\ GeV^2$ for E665 data, $0.1225 \le x \le 0.9055$ and $5.075\ GeV^2 \le Q^2 \le 5.925\ GeV^2$ for CLAS collaboration, and also $0.001 \le x \le 0.80$ and $1\ GeV^2 \le Q^2 \le 100\ GeV^2$ for NNPDF collaboration respectively.

In figures 1, we have plotted computed values of $F_2^d(x,t)$ against Q^2 values for x = 0.0045 and x = 0.008 considering k(x) = k, a constant and compared with NMC data. It is found that agreements of our results with data are best for $1.03 \le k \le 1.6$ in the entire range of our discussion.

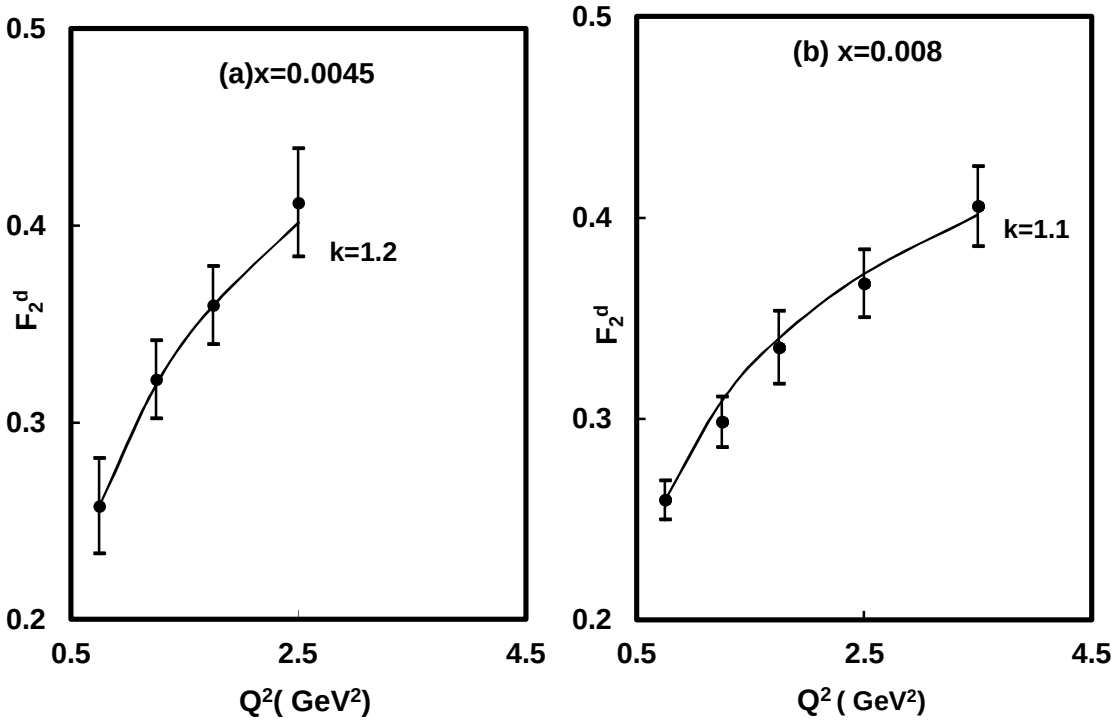

Figure 1: Comparison of t-evolution of deuteron structure function in LO with NMC data

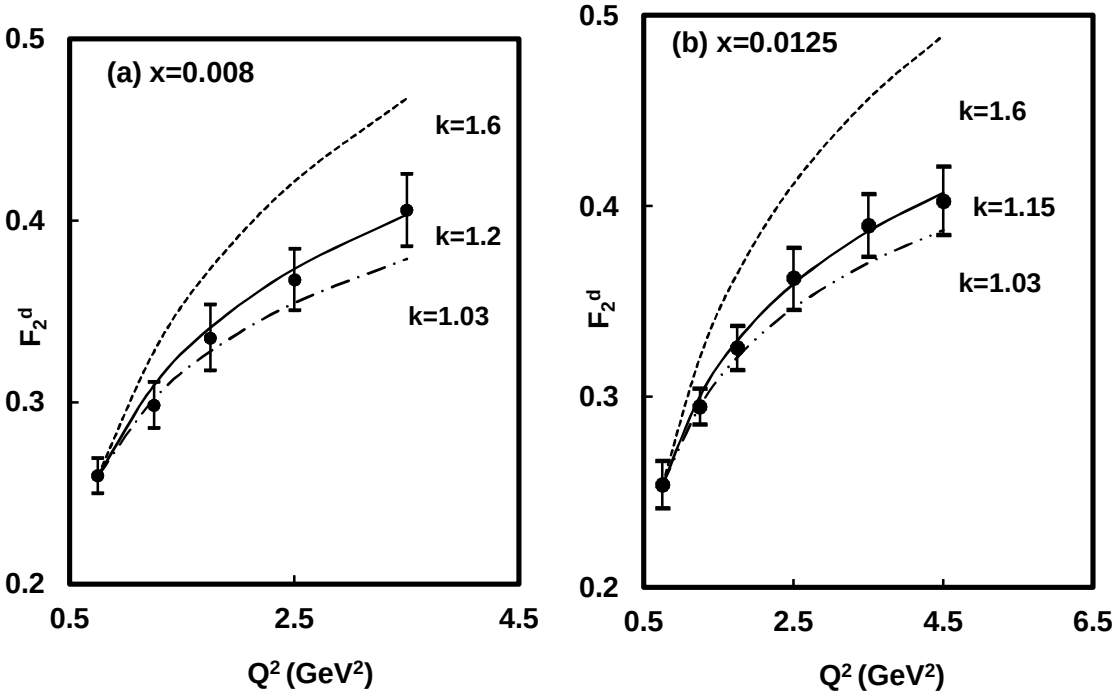

Figure 2: Sensitivity of parameter k in t-evolutions

In figures 3, for x-evolution, we have plotted computed values of $F_2^d(x,t)$ against the x values for a fixed Q^2 with considering k(x) = k, as a constant and compared with NMC data. Here we have plotted the graphs for Q^2 = 11.5 and 27 GeV^2 for the range of $0.025 \leq x \leq 0.14$. The best-fit curves get for the range of $1.0 \leq k \leq 1.3$ and as Q^2 increases the k value also increases.

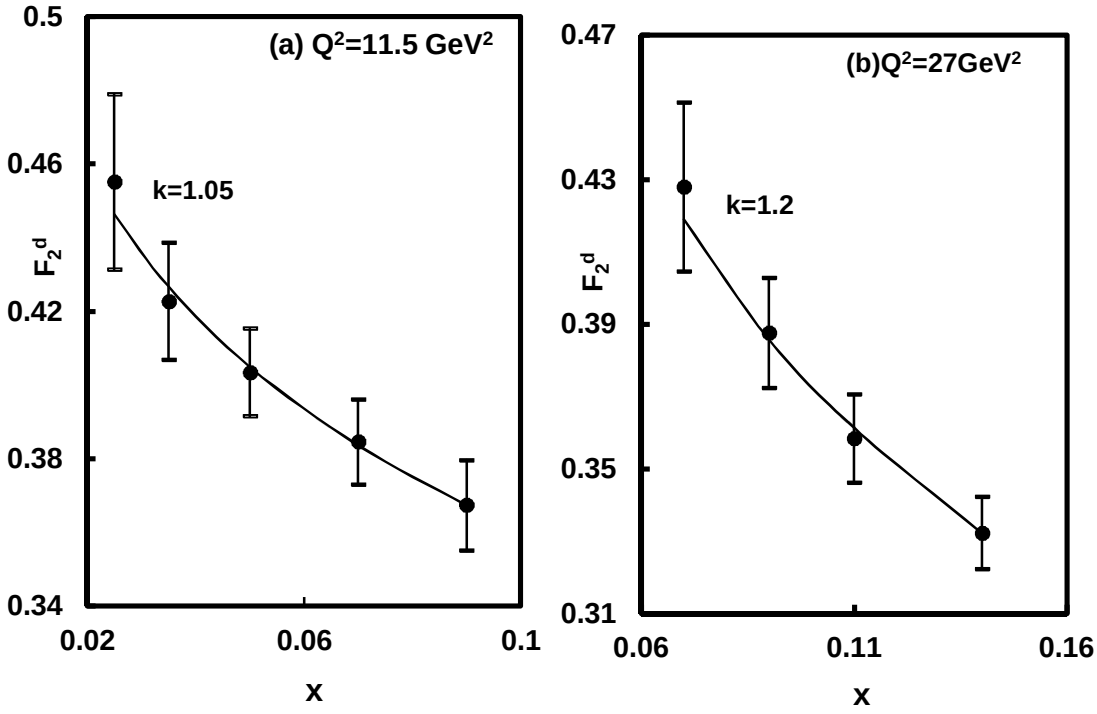

Figure 3: Comparing x-evolution of deuteron structure function in LO with NMC data

In figure 4, we have plotted computed values of $F_2^d(x,t)$ against the x values for a fixed Q^2 with k(x)=k, a constant and our results are compared with CLAS collaboration data. Though our theory on the DGLAP evolution equation are satisfied at high-Q^2 and small-x, but CLAS data are available at comparably smaller-Q^2 and higher-x. Thus our results are not properly satisfied with entire range of CLAS collaboration data. The best-fit curves are for $0.6 \leq k \leq 1.0$ with high-Q^2 and small-x ranges that available in CLAS collaboration.

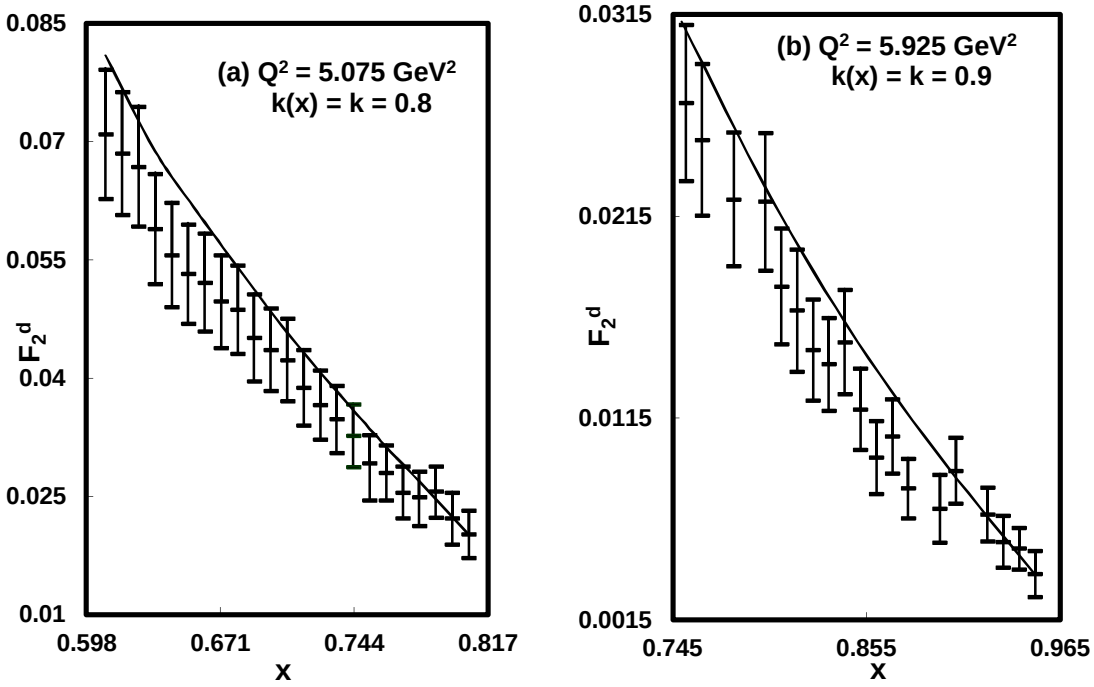

Figure 4: Comparing x-evolution of deuteron structure functions in LO with CLAS Collaboration data

In figures 5, we have plotted computed values of $F_2^d(x,t)$ against the Q^2 values for a fixed x and our results are compared with NNPDF collaboration data where the range of data used to train the 1000 nets which produced the results in ranges $0.003 \leq x \leq 0.8$; $0.5\ GeV^2 \leq Q^2 \leq 280\ GeV^2$ for the deuteron and non-singlet structure functions. Here we have considered k(x) = k, a constant and best-fit curves are for k = 1.1.

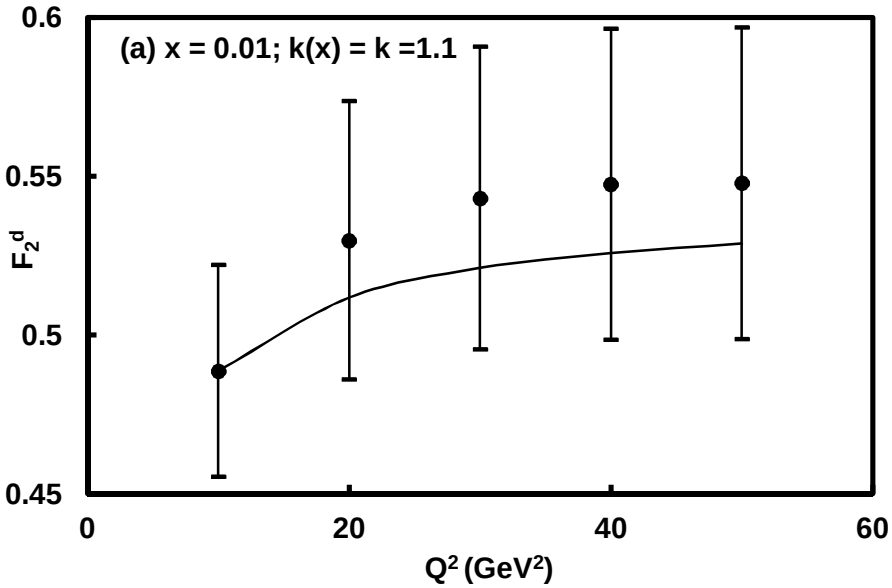

ISSN: 2321-9653; IC Value: 45.98; SJ Impact Factor: 7.429
Volume 8 Issue IV Apr 2020- Available at www.ijraset.com

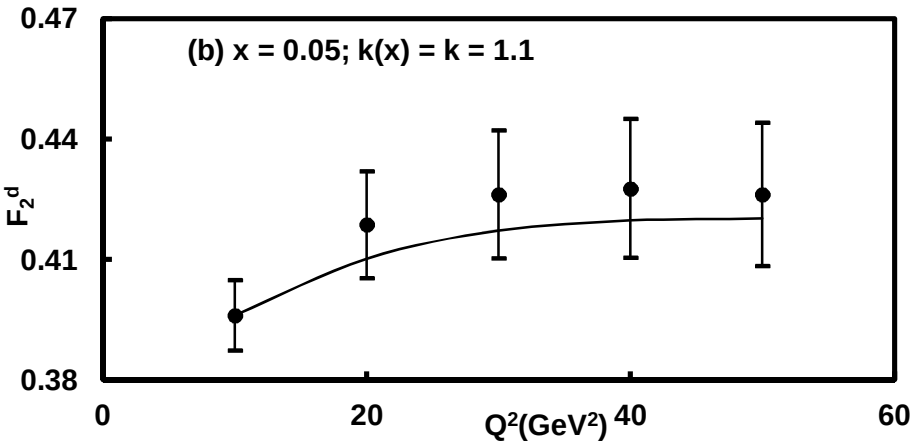

Figure 5: Comparing t-evolution of deuteron structure function in LO with NNPDF collaboration data

In figures 6, for x-evolution, we have plotted computed values of $F_2^d(x,t)$ against the x values for a fixed Q^2 with k(x) as a constant and our results are compared with NNPDF collaboration data. The best-fit curves are for k(x) = k = 1.2.

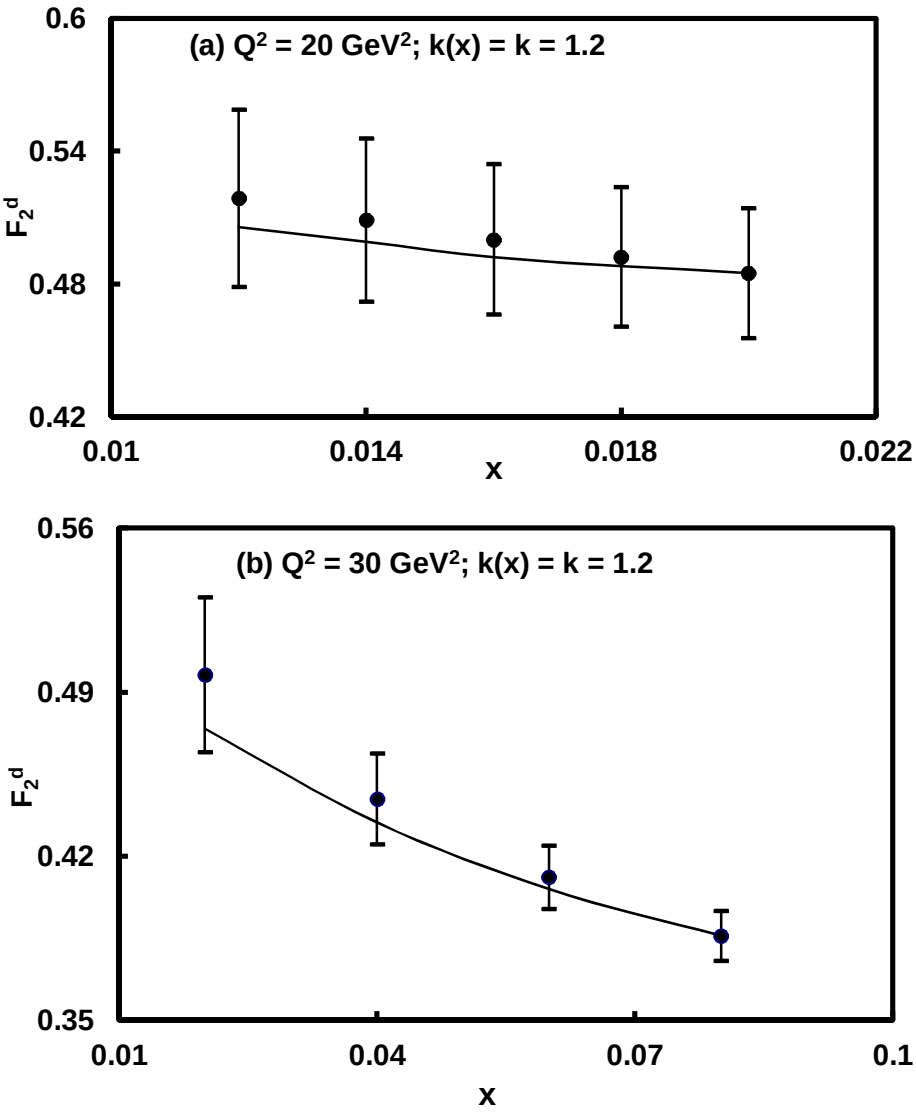

Figure 6: Comparing x-evolution of deuteron structure function in LO with NNPDF collaboration data

In figures 7, we have plotted computed values of $F_2^{NS}(x,t)$ against Q^2 values for fix values of x at 0.01, 0.017, 0.024, 0.035 for E665 data and at 0.0045, 0.008, 0.0125, 0.0175 for NMC data. The computed values are plotted against the corresponding values of Q^2 for the range from 1.496 GeV^2 to 13.396 GeV^2 for E665 data and from 0.75 GeV^2 to 7.0 GeV^2 for NMC data.

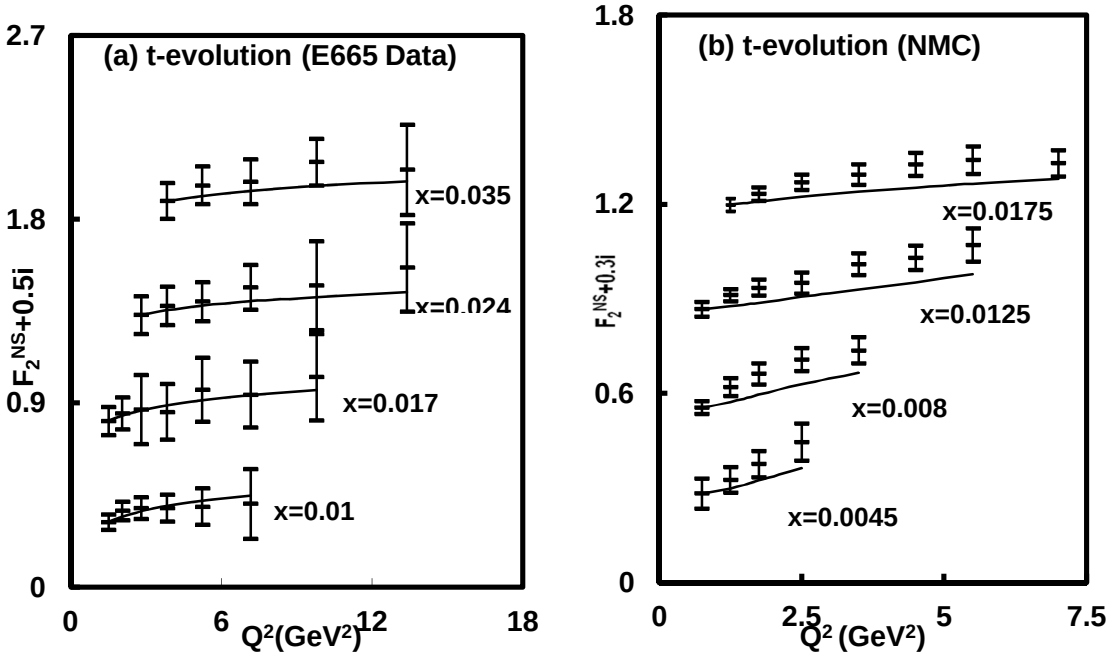

Figure 7: t- evolution of non-singlet structure functions in LO compared with E665 and NMC data. Value of each data point is increased by adding 0.5i and 0.3i, where i = 0, 1, 2, 3, …

In figure 8, the computed values of $F_2^{NS}(x,t)$ against x are plotted for fix Q^2 at 5.236 GeV^2, 7.161 GeV^2, 9.795 GeV^2, 13.391 GeV^2 for E665 data and at 9.0 GeV^2, 11.5 GeV^2, 15.0 GeV^2, 20.0 GeV^2 for NMC data. The data at highest values of x are taken as input values.

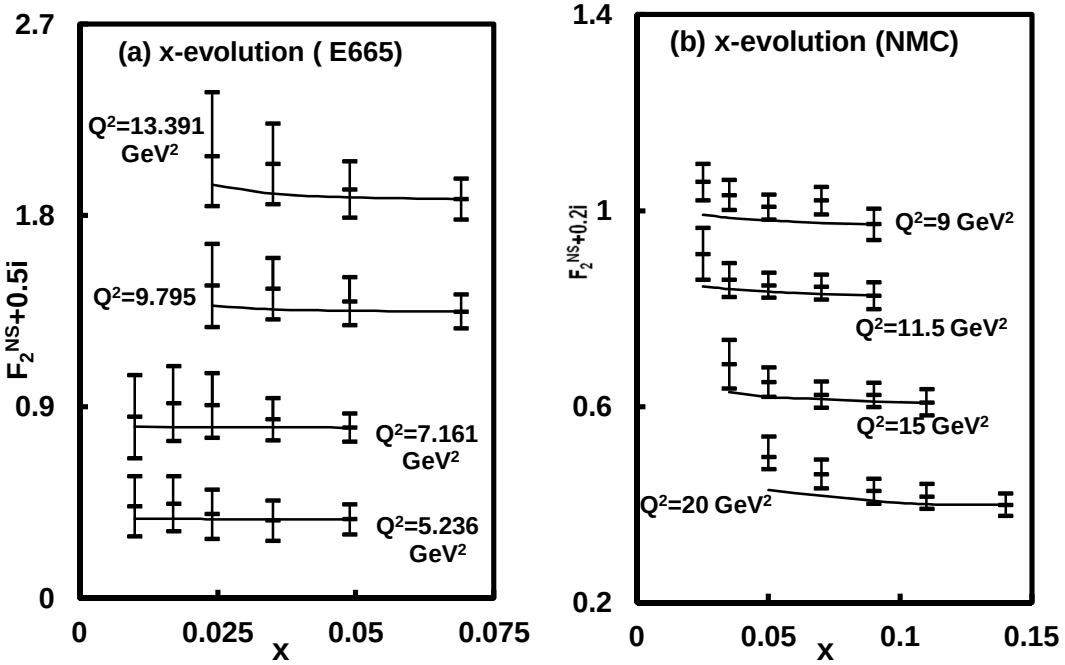

Figure 8: x-evolution of non-singlet structure functions in LO compared with E665 and NMC data. Value of each data point is increased by adding 0.5i and 0.2i, where i = 0, 1, 2, 3, …

III. CONCLUSION

The unpolarized DGLAP evolution equations have been solved for singlet and non-singlet structure functions in LO by using method of characteristics. Also have derived the t and x-evolutions of deuteron as well as non-singlet structure functions and results are compared with NMC, E665, CLAS collaboration data and NNPDF parameterization results. It is seen that structure functions increase as Q^2 increases from lower to higher values and decrease with x from higher to lower values. Results are in good agreement with these data sets especially at small-x and high-Q^2 region.

REFERENCES

[1] Gribov, V. N. and Lipatov, L. N. Soviet J Nucl Phys 15, 438 (1972)
[2] Lipatov, L. N. Soviet J Nucl Phys 20, 95 (1975)
[3] Dokshitzer, Y. Soviet Phys JETP 46, 641 (1977)
[4] Altarelli, G. and Parisi, G. Nucl Phys B 126, 298 (1977)
[5] Ball, R. D. and Forte, S. Phys Lett B, 335, 77 (1994)
[6] Kotikov, A. V. and Parente, G. Nucl Phys B 549, 242 (1999)
[7] Gehrmann, T. and Stirling, W. J. Phys Lett B 365, 267 (1996)
[8] Forte, S. and Ball, R. D. Acta Phys. Pol. B 26, 2087 (1995)
[9] Mankiewick, L., Saalfeld, A. and Weigl, T. Phys Lett B 393, 175 (1997)
[10] Neerven, W. L. van and Vogt, A. Phys Lett B 490, 111 (2000)
[11] Moch, S., Vermaseren, J. A. M. and Vogt, A. Nucl Phys B 688, 101 (2004)
[12] Moch, S. Vermaseren, J. A. M. Nucl Phys B 573, 853 (2000)
[13] Cafarella, A., Coriano, C. and Guzzi, M. Nucl Phys B 748, 253 (2006)
[14] Baishya, R. and Sarma, J. K. Phys Rev D 74, 107702 (2006); Phys Rev D 79, 034030 (2009); Indian J Phys 83, 1333 (2009); Eur J Phys C 60, 4 (2009); Eur J Phys C 72, 2036 (2012);
[15] Abbott, L. F., Atwood, W. B. and Barnett, R. M. Phys Rev D 22, 582 (1980)
[16] Altarelli, G. Phys Rep 18, 1 (1981)
[17] Sneddon, I. Elements of Partial Diff. Eq. (Mc Graw Hill, New York, 1957).
[18] Choudhury, D. K., Sarma, J. K. and Medhi, G. K. Phys Lett B 403, 139 (1997)
[19] Choudhury, D. K. and Sarma, J. K. Pramana J Phys 38, 481 (1997)
[20] R. Baishya, IJSR 9, 2 (2020)
[21] R. Baishya, IJRASET 9, III (2020)
[22] Baishya, R. and Sarma, J. K. Indian J Phys 83, 1333 (2009); Eur J Phys C 60, 4 (2009); Eur J Phys C 72, 2036 (2012)
[23] Farlow, S. J. Partial Diff. Eq. for Sc. and Eng. (John Willey, 1982)
[24] Arneodo, M. et al. CERN-NA-037, NMC, Nucl Phys B 483, 3 (1997)
[25] E-665 Collab, Adams, M. R. et al, Phys Rev D 54, 3006 (1996)
[26] CLAS Collaboration, Osipenka, et al. Phys Rev C 73, 045205 (2006)
[27] http://durpdg.dur.ac.uk/hepdata/online/f2/structindex.html
[28] http://www.sofia.ecm.ub.es/f2neural
[29] Forte, S., Garrido, L., Latorre, J. I. and Piccione, A. JHEP 05, 065 (2002)
[30] NNPDF Collaboration; Debbio, L. D. et al. JHEP 03, 080 (2005)
[31] BCDMS Collaboration; Phys. Lett. B 237, 592 (1990)
[32] Vogt, A. Comput Phys Commun 170, 65 (2005)

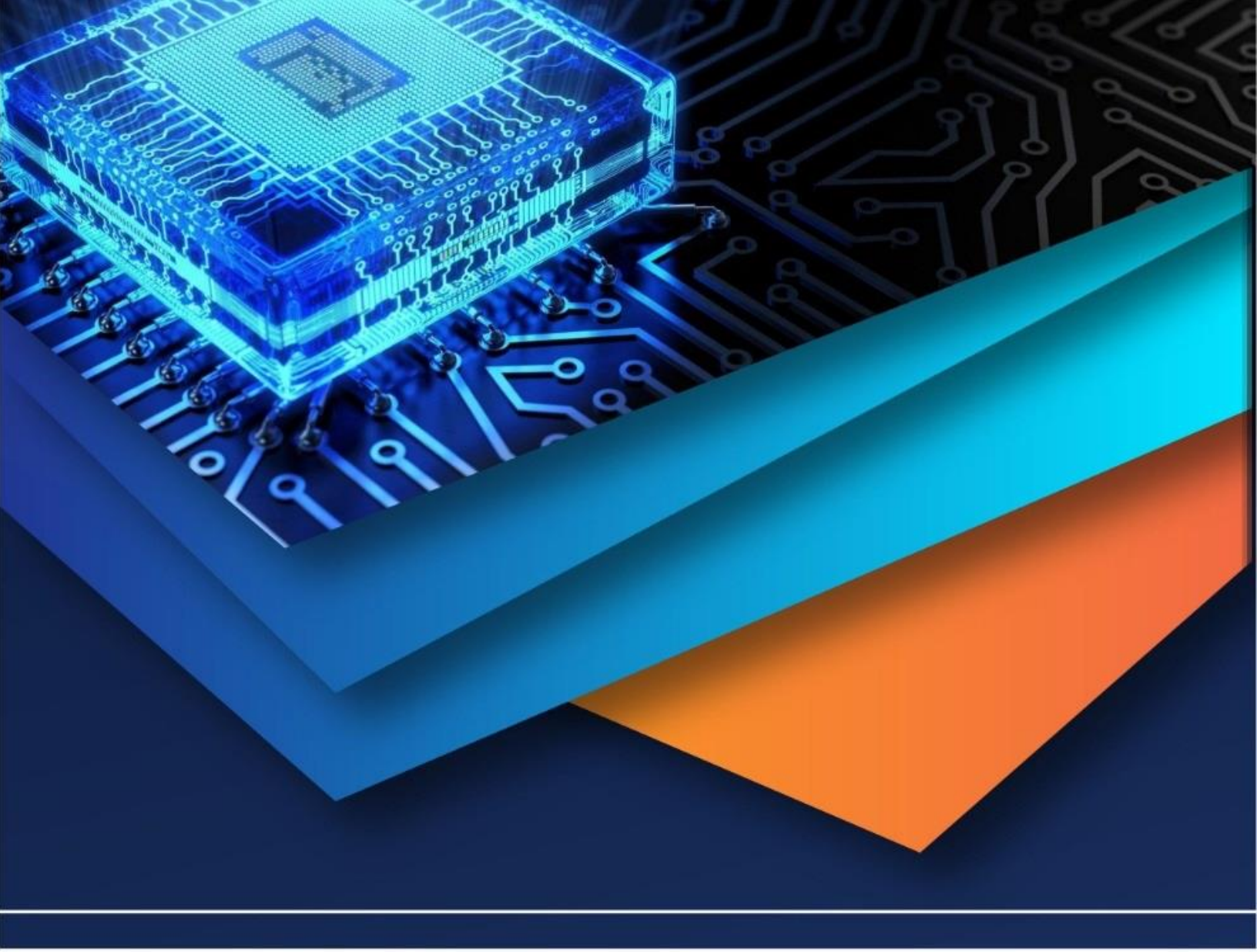

10.22214/IJRASET

45.98

IMPACT FACTOR: 7.129

IMPACT FACTOR: 7.429

INTERNATIONAL JOURNAL FOR RESEARCH

IN APPLIED SCIENCE & ENGINEERING TECHNOLOGY